Springback and Wrinkle Control in Deep Drawing of Paperboard with Segmented Blank Holder

Cédric Brunk ,* and Peter Groche

Deep drawing of paperboard enables highly productive forming processes for packaging products made of a recyclable material. However, the inherent anisotropy and low elasticity of paperboard pose challenges for deep drawing processes, especially resulting in direction-dependent springback and wrinkling of the formed parts. This paper presents an approach that addresses these challenges by using a segmented blank holder. The goal is to improve component quality both locally and globally by applying different blank holder forces to each segment. To this end, a concept is presented for a pneumatically driven segmented blank holder, along with two different forming geometries. Deep-drawing tests with segment-specific blank holder force distributions were performed and compared with those using a conventional blank holder. Although segmentation of the blank holder did not improve performance when the force per segment was identical, an uneven force distribution was able to improve forming in terms of shape accuracy and wrinkle pattern. Depending on the selected force distribution, significant compensation for springback anisotropy and the creation of wrinkle-free straight areas was shown to be possible.

DOI: 10.15376/biores.21.2.2832-2850

Keywords: Deep drawing; Paperboard; Segmented blank holder; Anisotropy; Wrinkling; Transparent tools

Contact information: Institute for Production Engineering and Forming Machines - PtU, Technical University Darmstadt, Otto-Berndt-Straße 2, 64287 Darmstadt, Germany;
** Corresponding author: cedric.brunk@ptu.tu-darmstadt.de*

INTRODUCTION

Although plastic packaging is the predominant solution for protecting and transporting consumer goods, it contributes significantly to global waste and pollution (Economist Impact and the Nippon Foundation 2021). Paper-based packaging is a promising solution because it is recyclable and biodegradable, and its raw materials are widely available. Various manufacturing processes have been developed and investigated for producing paper-based packaging. Casting processes enable the production of three-dimensional structures by filling a mold with a fiber suspension. However, the resulting packaging can be weak and exhibit a rough surface in the absence of further heating and pressing, thereby increasing production time and energy consumption. Folding cartons remain the most widely used solution, but they are usually limited to box-shaped geometries for mass-produced packaging. The production of more elaborate boxes requires complex folding machines and often the use of adhesive.

In the field of three-dimensional forming, media-based deep drawing can produce wrinkle-free components because shaping is largely achieved through stretching the material. For this purpose, the paper is clamped in the outer areas. Since paper has a low

stretchability, only shallow drawing depths are possible. Processes that allow the paper to flow into the forming zone enable greater drawing depths. Press forming, for example, can be used to produce deeper parts; however, wrinkles often occur and must be controlled by creasing.

Deep drawing has proven to be a particularly promising approach because it enables fast production of thin-walled packaging at cycle rates up to 150 cycles per minute (Hauptmann *et al.* 2017). In the deep drawing process, material from the clamped area between the die and the blank holder is drawn into the drawing gap between the die and the punch. Due to the reduction in diameter, material displacement occurs, leading to significant wrinkling in the paper. A key process variable is the blank holder force, which significantly influences the material flow and consequently the formation of wrinkles (Hauptmann *et al.* 2016). Due to its production process, industrial paperboard is an anisotropic material. It has higher strength but reduced elongation parallel to the fiber direction (machine direction, MD). The perpendicular direction is known as the cross direction (CD), where the strength is lower, but higher elongation is possible. This leads to direction-dependent forming behavior.

Previous research on optimizing wrinkle development and springback shows that the highest tolerable blank holder force and temperature lead to improved sample quality, especially regarding wrinkling (Müller *et al.* (2017). This can be combined with an optimized blank holder trajectory that is adapted to the maximum endurable load (Hauptmann *et al.* 2016). At the same time, increased blank holder forces may result in a slight decrease in shape accuracy due to anisotropic springback. Decreased shape deviation can be achieved by heating the forming tools (Wallmeier *et al.* 2016).

Various approaches to control material flow have been investigated in previous work and can generally be divided into influencing the raw material or advanced process control.

Several local material influences have been proposed in the past to improve the formability of paper in deep drawing. For instance, Groche *et al.* (2017) demonstrated improved formability of the material through localized heat application. Increasing the blank holder temperature in CD by 10 K compared to MD reduced the anisotropic springback compared to homogeneous temperature examples. Vogt and Hauptmann (2025) presented an approach in which multiple heating zones were integrated into a deep drawing tool. Although the possibility for a temperature variation between MD and CD is mentioned, the influence on the forming behavior is not described.

Additionally, the effect of localized steam application was analyzed. Franke *et al.* (2018) discovered that a higher moisture content in MD than in CD resulted in better shape accuracy for rotationally symmetric cups. Jessen *et al.* (2022) further investigated these results for rectangular geometry and various distribution patterns. Numerical and experimental approaches showed that adapting the moisture distribution to the geometry leads to a better product with more uniform wrinkle formation.

The influence of drawing beads is well established in metal forming and has also been investigated for paperboard forming. Jessen and Groche (2025) used drawing beads of different lengths and cross-sections that were parallel to the straight sections of a rectangular geometry. Through numerical and experimental validation, they demonstrated that greater drawing depths and local wrinkle control can be achieved.

In metal forming, the use of a segmented blank holder is established to influence material flow by specifically varying the local surface pressure. The variation of the force is typically achieved through an elastic blank holder and force transmission *via* several

parallel components. Hydraulic actuators are typically used for applying local forces, but alternative methods are also conceivable, such as electromagnets, as presented by Huang *et al.* (2023). An overview of the various actuators for controlling material flow in deep drawing, with a focus on metal forming, is provided by Allwood *et al.* (2016). Current research covers various force transmission methods, segment numbers, and arrangements. These methods allow for between two and 108 segments, some of which are arranged radially or around the circumference (Yagami *et al.* 2004; Zhang *et al.* 2021).

The use of a locally adapted blank holder force has not yet been studied for paper-based materials. Given the highly anisotropic properties of paper, adapting process control to the material's fiber direction seems promising. This paper presents a concept for actively influencing local surface pressure using a segmented blank holder based on pneumatic cylinders. The goal is to investigate the effects of segmentally decoupled and varying surface pressures on anisotropic springback and wrinkling in order to develop new methods for advanced paper deep drawing.

EXPERIMENTAL

Material

An industrial virgin fiber paper, Trayforma® from Stora Enso with a grammage of 350 g/m², was utilized in the investigations. It consists of three layers: a middle layer of chemi-thermomechanical pulp enclosed by two layers of chemical pulp (Storaenso 2025).

Two different moisture contents were examined. The paper was used after being stored under standard climate conditions (23 °C and 50% relative humidity), resulting in an equilibrium moisture content of approximately 6%. Additionally, a material moisture content of about 15% was considered. This was achieved by storing the material at 23 °C and 95% relative humidity for at least 12 hours. This significantly influenced the material's behavior. The higher moisture content increased the elongation from 2% in the machine direction (MD) and 5.5% in the cross direction (CD) to 2.5% (MD) and 7% (CD). At the same time, tensile strength decreased from approximately 60 N/mm² (MD) and 30 N/mm² (CD) to 48 N/mm² (MD) and 23 N/mm² (CD), as shown in Fig. 1.

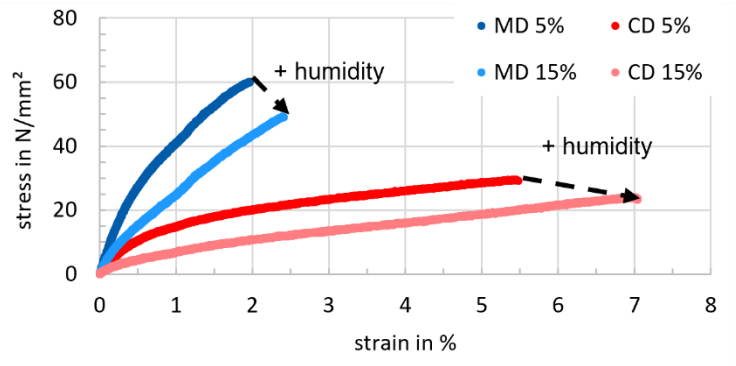

Fig. 1. Stress-strain diagram for paperboard stored under different conditions

Deep Drawing Setup

In the deep drawing of paperboard, the paper blank is pressed between the die and the blank holder. The paper is subsequently drawn into the die by the punch. In this study, the punch movement was performed by an electromechanical cylinder comprising a servo

motor with a linear axis. The blank holder force was applied by pneumatic cylinders. For using the conventional blank holder, four cylinders with a maximum total force of up to 25 kN were used. Alternatively, a segmented blank holder can be used; its design is described in more detail in the following subchapter. As presented in (Brunk and Groche 2025), the die was made of transparent acrylic glass, allowing the flange area to be viewed during the forming process. A centrally located, 12-megapixel camera continuously recorded and stored the forming process for later image-based evaluation.

The study examined two different geometries. A round punch with a 100 mm diameter was used as a basic shape to clearly demonstrate the effect of anisotropy. Additionally, a rectangular contour with edge lengths of 120 x 80 mm, whose corners were rounded with a radius of 20 mm, was used to focus on the effect of wrinkling in convex and straight areas. The drawing gap between the punch and die was 0.5 mm, and the punch had a conicity of 1° to counteract the increase in excess material as the drawing depth increases. The punches and dies both had a 3 mm radius at the bottom and inlet. Due to their high flexibility and low manufacturing costs, the punches were made of PLA.

The paper blanks used in the forming process were produced by laser cutting and have a diameter of 200 mm for the round geometry. For the rectangle geometry, the blank corresponds to a rectangle with edge lengths of 200 x 160 mm and corner rounding of 60 mm. The samples had an engraving in the center to mark the fiber orientation and ensure correct alignment and centering the sample within the system.

Segmented Blank Holder

The segmented blank holder consisted of individual elements that are arranged around the circumference with a 0.05 mm gap between segments. The force was applied by pneumatic cylinders mounted on a base plate. These cylinders were short-stroke cylinders with a low-friction configuration and a maximum stroke of 5 mm. In addition, the segments were guided by cylinder pins and slide bushings to prevent tilting.

Each cylinder was individually controlled by a proportional pressure regulator, enabling the segments to apply force independently. Due to the cylinders' 32 mm piston diameter and the available pressure range, forces of up to 643 N per cylinder were possible.

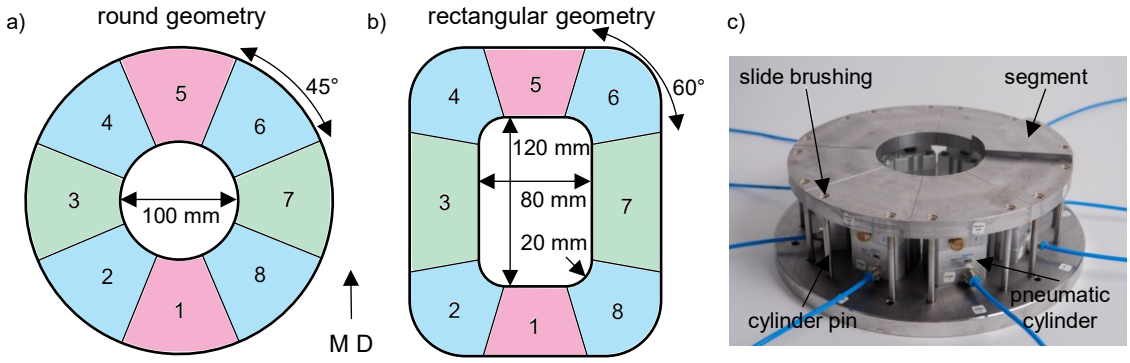

Fig. 2. Segmented blank holder used for a) round and b) rectangular geometries, segments with the same color are addressed at the same pressure in this study; c) shows the round segmented blank holder with one exemplary actuated segment

For the round geometry, the flange area was divided into eight equal segments, each of which covered an angle range of 45° (see Fig. 2a). With the given blank size, an initial surface pressure up to 0.219 N/mm² can be achieved per segment. The decrease in the flange area during deep drawing increased the maximum surface pressure that can be applied. Assuming that no stretching or material redistribution occurred for the specified geometry, the theoretical pressure was 1.455 N/mm² at the end of the process.

The rectangular geometry had eight segments of different shapes and sizes, as shown in Fig. 2b). The corner segments (segments 2, 4, 6, and 8) covered an angle of 60° and, compared to segment 1, had an area that was 1.047 times larger. The segments on the long edge (segments 3 and 7) had an area 1.795 times larger. Due to the larger surface area and to avoid tilting, two cylinders connected in parallel were used for these segments. With the specified paper blank sizes, maximum surface pressures of up to 0.324, 0.309, and 0.361 N/mm² were achieved in segments 1, 2, and 3, respectively, at the start of the process. At the end of the process, the theoretical maximum values increased to 1.596, 1.829, and 1.643 N/mm², respectively.

This study examined the influence of blank holder segmentation. First, it presents the impact of segmentation on deep drawing behavior when the same force is applied to all segments. It should be noted here that, for the rectangular geometry, an equal force per segment leads to different surface pressure per segment. Since the focus of this paper is on demonstrating the effects of segmentation, the process control was simplified so that the differences in segment area were not taken into account when applying the forces. For exactly the same surface pressure per segment, the actual surface area would have to be known at all times, which, as will be shown later, depends on the force and therefore cannot be determined in advance.

Additionally, different segment-wise variations of force levels were tested for round and rectangular contours as well as for dry and moist papers. During deep drawing, the force level remained constant for each segment. As already mentioned, this resulted in an increase in surface pressure as the remaining flange area decreased. The pressure increased by a factor of approximately 6.6 with the round geometry, while it increased by between 4.6 and 5.9 with the rectangular geometry, depending on the segment.

For rectangular geometries, testing began at 50 N per segment and increased by 25 N per segment until successful forming was no longer possible due to ruptures. This led to the force levels $\{50 + 25n | n \in \mathbb{N}_0\}$. Due to the higher attainable forces when forming the round geometry, force increments of 50 N (force-levels $\{50 + 50n | n \in \mathbb{N}_0\}$) and 100 N (force-levels $\{50 + 100n | n \in \mathbb{N}_0\}$) were tested for wet and dry samples, respectively. The force levels were identified in preliminary tests in order to achieve both good parts and failure limits for the respective geometries and material moistures with approximately 2 to 3 force levels, while keeping the scope of the tests manageable at the same time.

For reference, tests were conducted using a conventional blank holder. The same force levels are used, which correspond to the sum of the segment forces. For example, the force starts at $8x50N = 400N$ and increases in increments until failure, as described previously.

Next, the influence of varying control of the segments was examined. For this purpose, different force distributions across the circumference were investigated. Three different variants were examined for the round geometry:

- $V_{round}1$: A higher force level was selected in MD (segments 1 and 5) in order to place a greater load on the direction with the highest strength. The remaining segments were loaded at the same lower level.
- $V_{round}2$: A more even distribution across the circumference was examined with a higher force level in MD and a lower force level in CD (segments 3 and 7); the other segments in between at 45° were loaded at a medium level.
- $V_{round}3$: A combination of $V_{round}1$ and $V_{round}2$ was examined. To achieve this, the force level in the MD segment was increased by two levels compared to $V_{round}2$.

Three variations with different force distributions were also examined for the rectangular geometry.

- $V_{rect}1$: The straight sections (segments 2, 4, 6, and 8) experienced a higher force level than the corners.
- $V_{rect}2$: The straight sections were loaded at two force levels higher than the corners.
- $V_{rect}3$: A combination of $V_{rect}1$ and $V_{rect}2$ was used. The short segment oriented in MD (segments 1 and 5) was loaded with two force levels higher, while the segments in CD (segments 3 and 7) were loaded with one force level higher.

All force variations were examined by incrementally increasing the absolute forces until failure occurred, as previously described. Five repetitions were performed during all tests.

The segmented blank holder consists of individual segments with a 0.05 to 0.1 mm gap between them. This gap poses a risk of artificially initiating wrinkling and creating a preferred location for damage in the material. Occasional wrinkling was observed at segment transitions due to the gap and inconsistencies in the blank holder surface. Based on observation of the deep drawing process through the transparent die, there were no signs of rupture or material damage from the segmentation.

Quality Assessment

The geometric parameters were determined as the angular deviation of the wall from the vertical and the diameters of the semi-axes of the resulting component based on Hauptmann (2010), as shown in Fig. 3a. To record the geometric accuracy of the formed parts reproducibly, they were digitized using the laser scanner *Absolute Scanner AS1* as part of the *Hexagon Absolut Arm* and the *Inspire* software by Hexagon. Virtual cuts were made centrally along MD and CD in the point cloud and exported from the software for further processing (Fig. 3b). The contour of a virtual cut was then imported into *MATLAB* for further processing (Fig. 3c). First, a section of the point cloud was identified as belonging to the wall to calculate the angle. The starting point was set 10 mm above the bottom. The endpoint was then calculated by adding the desired draw depth minus 10 mm to the starting point. Finally, a linear fit (red line) was performed in the selected area to determine the angle to the horizontal. For each virtual cut (MD and CD), the angles on both sides were determined and averaged in each direction. In an ideal component without springback, a 90° angle was expected regardless of the forming geometry. For the round geometry, the anisotropy can be calculated using the MD/CD diameter ratio, with an ideal value of 1. The endpoint from the angle determination was also used to calculate the diameter and its deviation from the reference value.

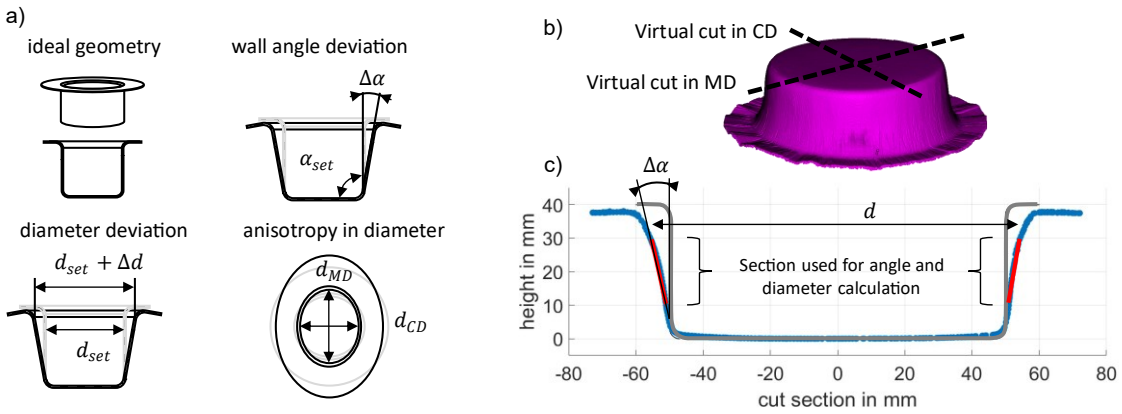

Fig. 3. a) Determination of geometric properties; b) example of scanned sample and c) derived geometric properties

In addition to determining the geometric properties, the wrinkles were recorded. They were manually counted after completion and removal of the formed parts for each segment and then averaged within similar segments and controls, as shown in Fig. 2a) and b) by identical colors.

RESULTS AND DISCUSSION

Control of Anisotropic Springback Behavior

Results for paperboard stored under standard conditions

The variations investigated for the round geometry when using samples stored under standard conditions are shown in Fig. 4.

Conventional	Segmented; same forces	Segmented $V_{round}1$	Segmented $V_{round}2$	Segmented $V_{round}3$
400 N	8 x 50 N F_{sum} = 400 N	MD: 150 N 45°: 50 N CD: 50 N F_{sum} = 600 N	MD: 250 N 45°: 150 N CD: 50 N F_{sum} = 1200 N	MD: 350 N 45°: 150 N CD: 50 N F_{sum} = 1400 N
1200 N	8 x 150 N F_{sum} = 1200 N	MD: 250 N 45°: 150 N CD: 150 N F_{sum} = 1400 N	MD: 350 N 45°: 250 N CD: 150 N F_{sum} = 1400 N	MD: 450 N 45°: 250 N CD: 150 N F_{sum} = 2200 N
2000 N	8 x 250 N F_{sum} = 2000 N	MD: 350 N 45°: 250 N CD: 250 N F_{sum} = 2200 N		MD: 550 N 45°: 350 N CD: 250 N F_{sum} = 3000 N
2800 N	8 x 350 N F_{sum} = 2800 N	**Variants of distributed forces** $V_{round}1$: MD-segments (Segment 1 and 5) increased by 1 force level compared to other segments $V_{round}2$: MD-segments increased by 1 force level compared to segments under 45°; CD-segments (Segment 3 and 7) reduced by 1 force level $V_{round}3$: MD-segments increased by 2 force levels compared to segments under 45°; CD-segments reduced by 1 force level		**Scoring** based on number of rupture-free formations in 5 reps. Success (4 or 5) Partly success (2 or 3) Failed (0 or 1) not tested
3600 N	8 x 450 N F_{sum} = 3600 N			
4400 N	8 x 550 N F_{sum} = 4400 N			

Fig. 4. Summary of formability using conventional and segmented blank holders for round geometry and with paperboard stored under standard conditions

The columns display the various options for controlling the segmented blank holder, in addition to the conventional blank holder, which consists of a single solid part.

The incrementally increased force levels of 100 N are shown in the rows. The color coding shows whether forming was possible at a drawing depth of 40 mm. Green indicates that one out of five repetitions cracked at most, while red shows that at least four out of five repetitions ruptured. Force levels shown in yellow indicate a transition zone in which two or three out of five samples were successfully transformed. Higher force levels were not tested if the lower force level was marked red.

When using the round geometry with paper stored under standard conditions, it is apparent that the segmentation of the blank holder only allows for lower blank holder forces to be achieved when comparing the total force to the conventional blank holder. This can be explained by the fact that the segmentation results in a more uniform surface pressure across the entire flange. During deep drawing with a conventional blank holder, most wrinkles form in the MD, as also presented in (Brunk and Groche 2025). The formation of these wrinkles increases the distance between the blank holder and the die, leading to an uneven distribution of surface pressure. In areas with wrinkles (mainly along MD), the local surface pressure increases, while in areas without wrinkles (mainly along CD), it decreases due to the lower effective material thickness. This has a positive effect on the process due to the material's higher load-bearing capacity in MD. When using a segmented blank holder, the force applied to each segment is decoupled from the forces applied to the others. The formation of wrinkles along MD, therefore, does not result in a decrease in surface pressure in CD. Despite the mathematically identical total load, failure occurs earlier in CD because the material's tensile strength is exceeded locally.

As previously described, the segmented blank holder enables the active exploitation of different load capacities through the controllability of each segment, which may prove to be profitable. In variations $V_{round}1$ to $V_{round}3$, higher forces were applied to the MD segments. In $V_{round}1$, only the MD segments are loaded at a higher force level. This allowed for a higher total force to be achieved than with segmentation, where all segments had an identical force. In $V_{round}2$, a uniform progression from MD over 45° to CD was used. Although the total force was the same here as in $V_{round}1$, it can be seen that the increased force in the 45° and CD compared to $V_{round}1$ led to failure (see row 2). Due to the transparent die, it is visible that the rupture began in the 45° segment, which is atypical for failure. This was counteracted in $V_{round}3$ by increasing the MD force level further. Here, the MD segments were set three force levels higher than CD, while the 45° segments were one force level higher than the CD segments. The lowest force level could be formed without rupture; however, starting from the second force level, rupture occurred and initiated in the MD direction. This indicates that the load redistribution shifted the failure zone from CD in conventional deep drawing to MD.

Comparing $V_{round}1$, $V_{round}2$, and $V_{round}3$ to the segmented blank holder with the same force levels shows, that load redistribution with increased forces toward the MD-segment significantly affected formability. While failure occurred at a force of 150 N in the CD-segment with $V_{round}2$, at least partly successful drawing could be achieved by increasing the force in the MD-segment without changing the force in the CD-segment.

The decoupling of the segments also is shown in Fig. 5, displaying the distances between the die and blank holder over the drawing depth. The solid blank line corresponds to the conventional blank holder. The distance increased, starting at about 5 mm, where the first wrinkles occurred, up to about 0.8 mm. This corresponds to almost two times the material thickness of 0.465 mm. Towards the end of the process, the distance was about the same as the material thickness. The colored solid lines show the distances for the segments in MD, 45°, and CD, for the segmented blank holder with the same forces for all

segments. Here, the MD-segment showed a very high thickness change, as wrinkles form mainly parallel to MD. The segments in 45° and CD were decoupled and showed a decrease in distance at the beginning of the process. This can be attributed to a compression in the thickness direction due to the blank holder force. At a draw depth of about 18 mm, the distance increased again due to wrinkles, but they stayed low compared to the MD-segment. Additionally, the variation $V_{round}2$ is shown with dotted lines. In $V_{round}2$, the MD-segment was subjected to a higher force, whereas the CD-segment had a lower force. This influenced the change in thickness, resulting in the CD-segment showing the highest increase. This was due to the formation of very coarse wrinkles, which will be discussed further below. The MD-segment, which experienced higher force, showed less change in distance, resulting in the formation of finer wrinkles.

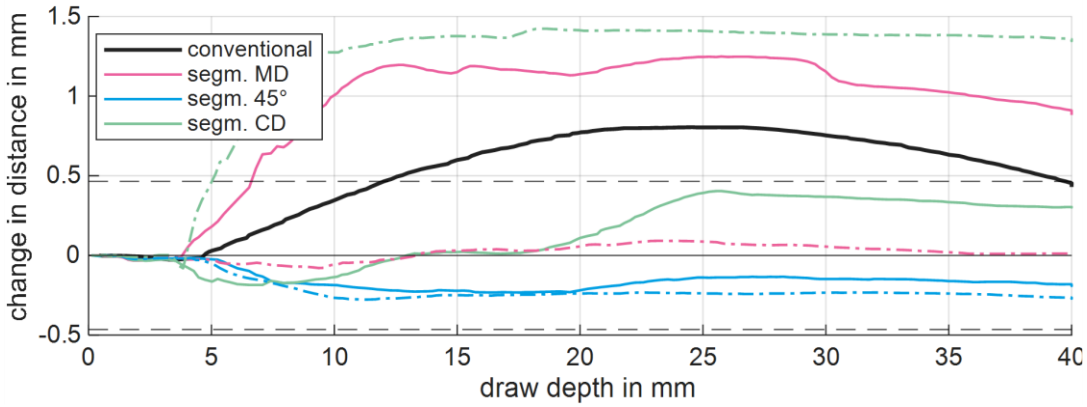

Fig. 5. Change in distances between die and blank holder for conventional blank holder (black line) and for segmented blank holder with same forces per segment (MD, 45° and CD, with solid line) and $V_{round}2$ (dotted line); the horizontal dashed black line shows the initial material thickness

Figure 6a) shows the anisotropy and springback of the samples after removal and analysis using the aforementioned method. For the conventional blank holder, the anisotropy ratio (the diameter in MD divided by the diameter in CD) was always greater than 1, which indicates ovality with the longer axis parallel to the MD.

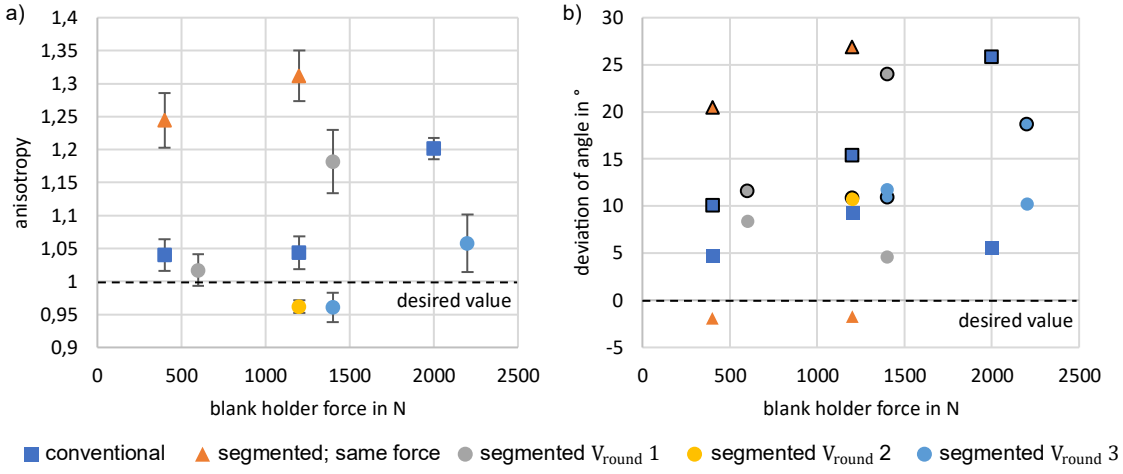

Fig. 6. a) Anisotropy with standard deviation in round dry samples during deep drawing with conventional and segmented blank holder, and b) springback in MD and CD; MD values with black border

Segmenting the blank holder with the same force in each segment led to a significant increase in anisotropy. With distributed loading of the segments, the results varied depending on the variant. With variant $V_{round}1$, slight compensation of the anisotropy could be achieved, though some ovality remained. Variants $V_{round}2$ and $V_{round}3$ at the first force level resulted in an anisotropy value of less than 1. The possibility of reversing anisotropy demonstrates that complete compensation was feasible by adjusting the load on each segment.

In addition to anisotropy, absolute springback is also important for achieving high dimensional stability. Ideally, the springback angle is 0°. Springback in the MD and CD directions is plotted individually for each variation examined in Fig. 6b). To distinguish between the two directions, the MD is marked with a black border. The standard deviation was omitted for improved readability. As shown in the diagram, for the conventional blank holder, springback in the MD direction increased with increasing blank holder force. This was also evident when the blank holder was segmented and loaded with an identical force per segment. The wall angle deviation in CD was negative for the segmented same force variant, because the wall angle was lower than 90°. Uneven loading of the segments results in low springback in both directions, especially for variant $V_{round}2$. Within the scope of the variations considered, $V_{round}2$ (with a total force of 1200 N) and $V_{round}3$ (with a total force of 1400 N) were the most promising variants for low and uniform springback with anisotropy close to 1.

The reduced and more uniform springback during load distribution over the blank holder resulted from a change in the wrinkle pattern, as already mentioned above (see Fig. 5). Additionally, Fig. 7 on the left shows the wrinkle pattern for a deep-drawn sample with a conventional blank holder and a force of 1200 N, in both top and CD side views. Due to the low material moisture content, only a low number of about 50 coarse wrinkles appeared. In comparison, the image on the right shows a sample of variant $V_{round}3$ with a total force of 1400 N. This sample had an anisotropy of less than 1, and more wrinkles formed. However, due to the low blank holder force of 50 N in the CD-segment, the wrinkles formed here were very coarse and overlap heavily, absorbing a large proportion of the excess material.

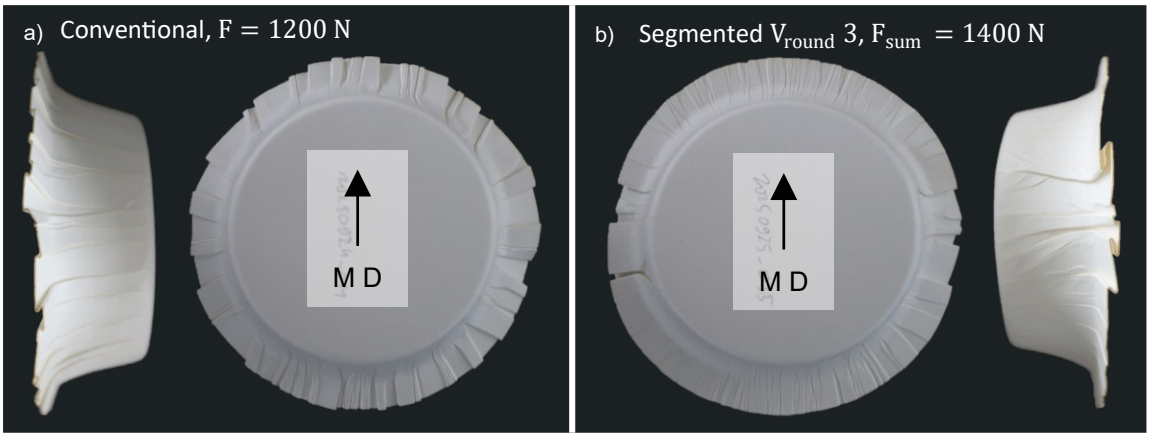

Fig. 7. Examples for wrinkling in round dry samples during deep drawing with conventional and segmented blank holder, top-view and sideview

Results for paperboard with increased humidity

Due to their superior shape and wrinkling properties, papers with 15% moisture content were also examined. Since the strength decreases with higher material moisture, lower force levels can be used. Therefore, force increments of 50 N were investigated. Pure segmentation, in which all segments are subjected to the same force, leads to a low usable maximum force. The failure occurred in the CD-segment at a load of 100 N. Surprisingly, in configuration $V_{round}1$, where the segments in MD and 45° are subjected to a higher load, the 100 N in the CD-segment was possible without cracking.

Conventional	Segmented; same forces	Segmented $V_{round}1$	Segmented $V_{round}2$	Segmented $V_{round}3$
400 N	8 x 50 N F_{sum} = 400 N	MD: 100 N 45°: 50 N CD: 50 N F_{sum} = 500 N	MD: 150 N 45°: 100 N CD: 50 N F_{sum} = 800 N	MD: 200 N 45°: 100 N CD: 50 N F_{sum} = 900 N
800 N	8 x 100 N F_{sum} = 800 N	MD: 150 N 45°: 100 N CD: 100 N F_{sum} = 900 N	MD: 200 N 45°: 150 N CD: 100 N F_{sum} = 1200 N	MD: 250 N 45°: 150 N CD: 100 N F_{sum} = 1300 N
1200 N	8 x 150 N F_{sum} = 1200 N	MD: 200 N 45°: 150 N CD: 150 N F_{sum} = 1300 N	MD: 250 N 45°: 200 N CD: 150 N F_{sum} = 1600 N	
1600 N	8 x 200 N F_{sum} = 1600 N			
2000 N	8 x 250 N F_{sum} = 2000 N			

Fig. 8. Summary of formability using conventional and segmented blank holders for round geometry and with paperboard with 15% humidity

As shown in Fig. 9, the anisotropy value for deep drawing moist samples with a conventional blank holder was approximately 1.05 and did not clearly depend on the blank holder force. The angular deviations showed again that MD had a higher springback, but both angles were not clearly dependent on the blank holder force.

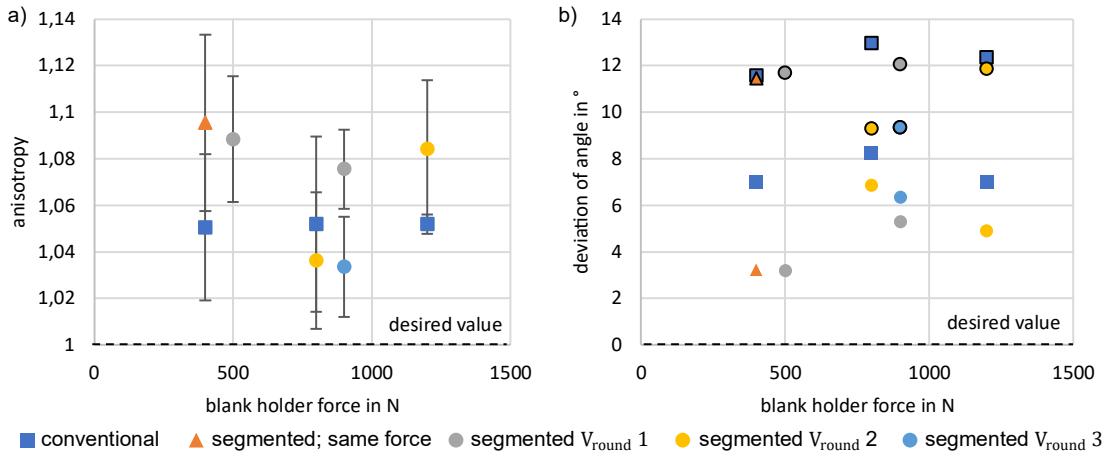

Fig. 9. a) Anisotropy and b) springback in round humid samples during deep drawing with conventional and segmented blank holder; MD values with black border

For segmentation with the same force level, the anisotropic behavior became more pronounced. Among all the test runs with force distribution across the segments, variants $V_{round}2$ and $V_{round}3$ at the lower force level exhibited the least angle deviation in MD and CD, with minimal differences between them. This was reflected in the anisotropy value close to 1, but complete compensation of anisotropy with a value of 1 was not achieved for wet samples in deep drawing. Nevertheless, with regard to the standard deviation, the influence of the segmented blank holder on anisotropic springback was subject to further significant deviations, such as the inhomogeneous material structure.

Figure 10 shows the wrinkle pattern for moist samples during deep drawing with a conventional blank holder, as well as for variation $V_{round}3$, which had a similar total blank holder force. As is typical with moistened paper, the wrinkle pattern was significantly finer. However, when comparing variation $V_{round}3$ to the conventional blank holder, the formation of coarse wrinkles in the CD-segment can be seen.

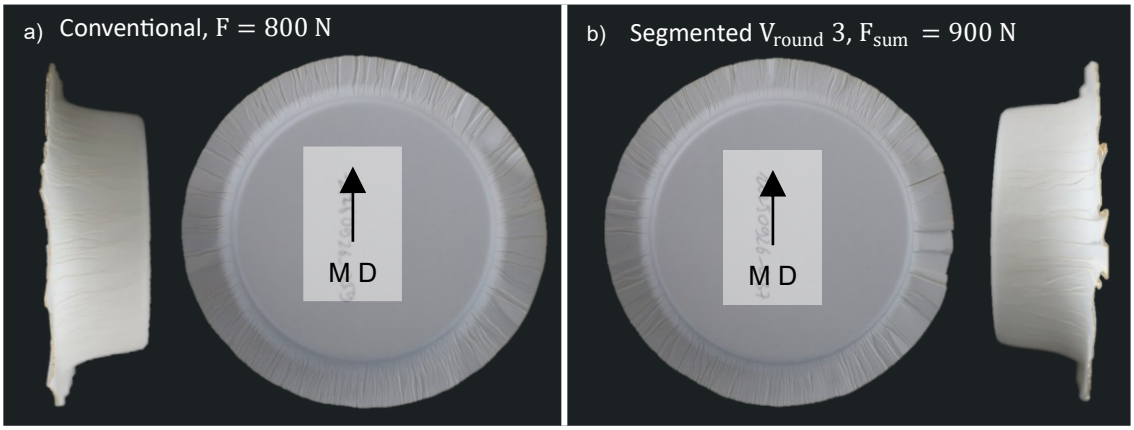

Fig. 10. Examples for wrinkles in round moist samples during deep drawing with conventional and segmented blank holder, top-view and sideview

Discussion of Anisotropic Springback Behavior

Using a segmented blank holder for deep drawing led to a worsening of anisotropic springback and wrinkling when the same forces were applied to all segments. This effect was evident in both samples stored under standard conditions and moist samples.

In contrast, using a segmented blank holder with directionally adjusted forces influenced the anisotropic springback. Due to paper's higher strength parallel to the MD, a higher blank holder force can be applied there. Depending on the distribution of the local force, the anisotropic behavior of springback can be influenced. In the case of dry paper, it can be completely compensated, depending on the parameters. The improved roundness of the samples was partly due to a significant reduction in wrinkling quality in the CD area. However, this was also due to large differences in force levels between the segments. The effects of reduced anisotropy and associated wrinkling deterioration were more pronounced in dry samples than in moist samples. This can be attributed to the coarser wrinkling in the dry samples, which resulted in a more inhomogeneous local surface pressure.

Overall, the results showed that for a rotationally symmetrical part, the anisotropy of springback can be actively influenced — albeit at the cost of a degraded wrinkle pattern. This reveals a controllable trade-off between the target variables "(an)isotropy of springback" and "fine and homogeneous wrinkling."

The influence on anisotropy was comparable to that reported by Groche *et al.* (2017) using local temperature control. A difference of 10 K between MD and CD resulted in a 3% improvement in anisotropy.

Control of Wrinkle Behavior

Results for paperboard stored under standard conditions

Figure 11 shows the force variations examined for the rectangular geometry. As the rounded corners of the rectangle are critical areas at higher drawing depths, a depth of 30 mm was used in the following section. The force increments examined were 25 N per segment.

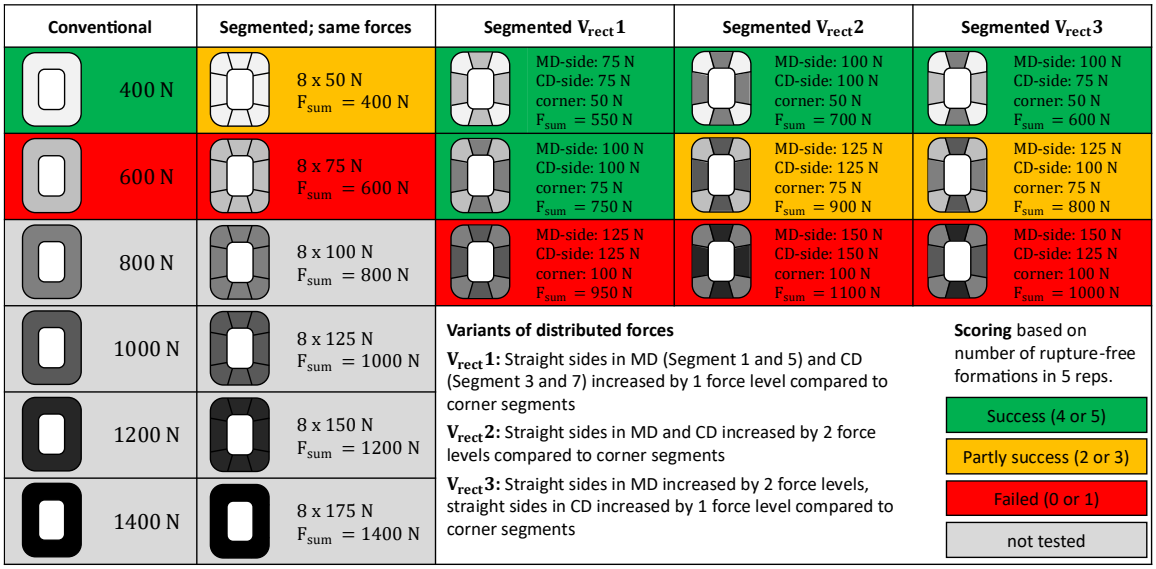

Fig. 11. Summary of formability using conventional and segmented blank holders for rectangular geometry and with paperboard stored under standard conditions

Similar to the round geometry, segmentation of the blank holder caused deterioration in forming at higher forces when the total force per segment was identical. Although the same force was applied, the larger surface area of the long side resulted in a surface pressure that was approximately half that of the short edge and corner areas. Compared to the conventional blank holder, this resulted in a significant local reduction in surface pressure, which negatively affected formability.

In variant $V_{rect}1$, the straight sections increased by one force level (25 N). This equalizes the surface pressure in the corner and the long straight section, though the corner areas still exhibited slightly higher surface pressure. The highest surface pressure was still found in the short edge area. This is advantageous for forming, as it allows for a higher total force of the segments in deep drawing than when using a conventional blank holder. In variant $V_{rect}2$, the surface pressure between the long edge and the corners was evened out, which also allowed for greater total blank holder forces than with a conventional blank holder. In variant $V_{rect}3$, the load on the short edge was increased further. However, this resulted in earlier failure due to cracks in the corner areas compared to $V_{rect}1$.

Unlike a round contour, a rectangular contour does not result in excess material everywhere, as straight sections do not increase material surplus. However, wrinkles still appeared on the straight sections of rectangular contours. This can be seen in the samples

examined in the case of the conventional blank holder. As shown in Figure 12, an average of about two wrinkles occurred in the area of the long edge, while an average of about four wrinkles occurs in the area of the short edge. The higher number of wrinkles on the short edge compared to the long edge can be explained by the orientation of the paper. Due to anisotropy, more wrinkles generally occur parallel to the MD. On average, five wrinkles were present in the corner areas.

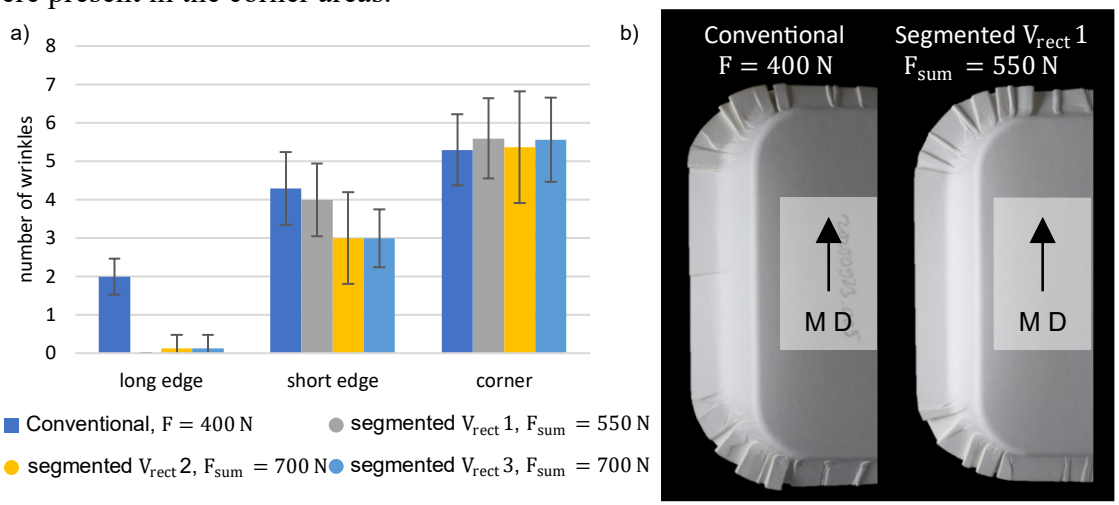

Fig. 12. Number of manually counted wrinkles in the geometric sections of the rectangular parts for dry samples and examples for the conventional blank holder and $V_{rect}1$

Using the segmented blank holder significantly influenced the wrinkle pattern. In all variants ($V_{rect}1$ to $V_{rect}3$), a reduction in wrinkles was evident in the area of the long edge. In particular, $V_{rect}1$ had a completely wrinkle-free area over the entire 90 mm length of the segment (Fig. 12b). In the area of the short edge, there was a slight reduction in the number of wrinkles, though they were not entirely prevented. This was due in part to the shorter edge length (45 mm) and the material alignment. The slight reduction was due to the increased local surface pressure compared to the conventional blank holder. Although changes in the number of wrinkles were visible in the straight segments, there was no clear influence on the wrinkles in the corner area.

Results for paperboard with increased humidity

Figure 13 shows the force levels examined for wet paper with a moisture content of 15% using the rectangular die. The increased moisture allows for higher blank holder forces due to improved wrinkling. When the blank holder is segmented with the same forces per segment, the change in local pressure causes failure at a total force of 600 N, whereas this force leads to successful forming when using the conventional blank holder. When loads are distributed unevenly, a total blank holder force comparable to the maximum force when using the conventional blank holder can be applied.

Figure 14a) shows the resulting wrinkles for the tested configurations. Due to increased material moisture, more wrinkles are visible across all tests. For the force range shown, the conventional blank holder produced an average of nine wrinkles on the straight edge, while variations $V_{rect}1$ to $V_{rect}3$ reduced this number to around four. The number of wrinkles on the short edge could also be reduced from around 19 to between seven and 13. As Figure 14b) shows, the wrinkles had a different appearance, particularly on the long edge. With the conventional blank holder, fully developed wrinkles with partial material

overlap were visible. In contrast, only slight imperfections on the material could be seen when using the segmented blank holder. These imperfections can be assessed as the beginning of a wrinkle, though not a fully pronounced one. These beginnings of wrinkles were nevertheless counted as wrinkles in the evaluation, resulting in a count of more than none wrinkle in the area of the long edge. Without evaluating these imperfections, the area would appear completely wrinkle-free. There was also a slight reduction in the number of wrinkles in the corners. In variants $V_{rect}1$ to $V_{rect}3$, the blank holder force in the corner segments was lower than with the conventional blank holder, despite the overall force being comparable. This is evident from the slightly coarser appearance of the wrinkles in the corner areas compared to those with the conventional blank holder.

Conventional	Segmented; same forces	Segmented $V_{rect}1$	Segmented $V_{rect}2$	Segmented $V_{rect}3$
400 N	8 x 50 N F_{sum} = 400 N	MD-side: 75 N CD-side: 75 N corner: 50 N F_{sum} = 550 N	MD-side: 100 N CD-side: 100 N corner: 50 N F_{sum} = 700 N	MD-side: 100 N CD-side: 75 N corner: 50 N F_{sum} = 600 N
600 N	8 x 75 N F_{sum} = 600 N	MD-side: 100 N CD-side: 100 N corner: 75 N F_{sum} = 750 N	MD-side: 125 N CD-side: 125 N corner: 75 N F_{sum} = 900 N	MD-side: 125 N CD-side: 100 N corner: 75 N F_{sum} = 800 N
800 N	8 x 100 N F_{sum} = 800 N	MD-side: 125 N CD-side: 125 N corner: 100 N F_{sum} = 950 N	MD-side: 150 N CD-side: 150 N corner: 100 N F_{sum} = 1100 N	MD-side: 150 N CD-side: 125 N corner: 100 N F_{sum} = 1000 N
1000 N	8 x 125 N F_{sum} = 1000 N	MD-side: 150 N CD-side: 150 N corner: 125 N F_{sum} = 1150 N		
1200 N	8 x 150 N F_{sum} = 1200 N			

Fig. 13. Summary of formability using conventional and segmented blank holders for rectangular geometry and with paperboard with 15% humidity

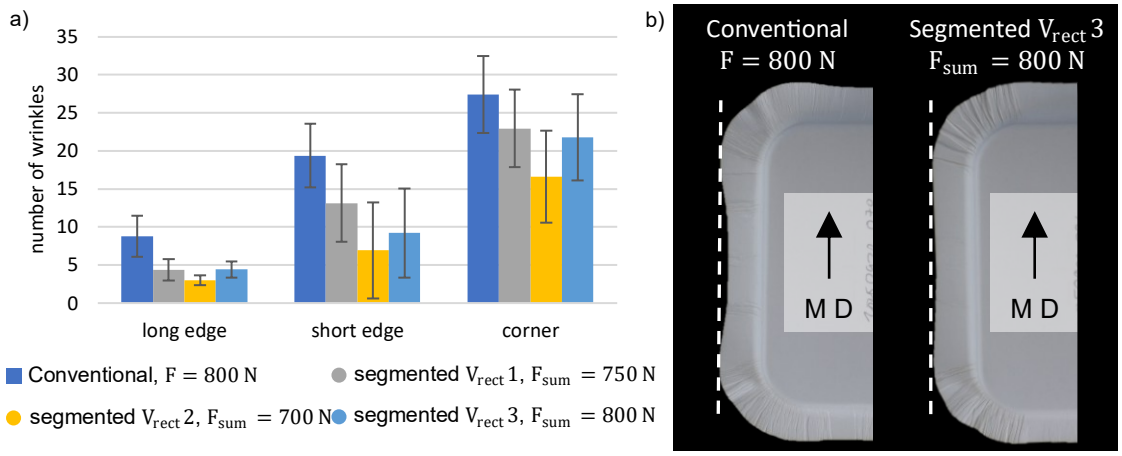

Fig. 14. Number of wrinkles in the geometric sections of the rectangular parts for moist samples and examples for the conventional blank holder and $V_{rect}3$

Another noticeable feature when examining the formed samples using the conventional blank holder is the visible narrowing in the straight sections, resulting in varying remaining flange lengths. This was again due to the higher surface pressure in the corner areas. Material flow was impeded at the corners, which required greater elongation and left a longer flange. Due to the low surface pressure, simplified material feed was

possible in the straight sections, which reduced the remaining flange length. When the blank holder was segmented and a higher force was applied to the straight sections, the remaining flange length increased due to greater elongation resulting from the more hindered material feed.

Figure 15 shows the wall angles in MD and CD for the force variations examined for the segmented and conventional blank holders. Like the rotational symmetric geometry, the wall angles in MD (short edge area) were larger than in CD. The segmented blank holder significantly reduced the springback angle in MD for all variants examined and slightly decreased it in CD.

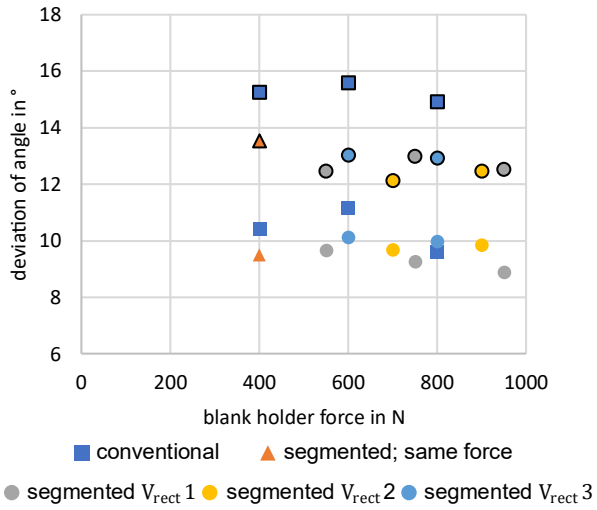

Fig. 15. Springback for rectangular moist samples during deep drawing with conventional and segmented blank holder; MD values with black border

Using a segmented blank holder has great potential to influence wrinkling in rectangular geometries when selecting a segment-specific blank holder force. For the rectangular geometry considered, the wrinkling was able to be significantly improved, especially in the straight sections, while springback was simultaneously reduced. Within the scope of the variations examined, it was shown that higher force in straight sections compared to the corner areas led to better wrinkling in dry and wet samples. Depending on the force distribution chosen, a wrinkle-free area could be achieved. The observed effects on the wrinkle pattern were more pronounced with dry samples than with wet samples. Additionally, a uniform flange pull-in could be achieved with locally adjusted blank holding forces.

The results for the rectangular geometry were comparable to those obtained with draw beads, as investigated by Jessen and Groche (2025) for a rectangular contour. The use of drawing beads showed a comparable effect with wrinkle-free straight sections, an influence on the wrinkle pattern in the corners, and on the remaining flange length.

Outlook

Thus far, the investigation of the segmented distribution of blank holder forces has been based on a simple metric, with force levels changing in fixed increments. To clearly see the effects of segmentation, the differences between segments were chosen to be large. For further investigations, this simple approach should be replaced by an analysis of

surface pressure levels, especially for a contour in which not all segment areas are the same size. Such an approach can allow for a better comparison of the effects on the forming process. Additionally, the distribution should be adapted to geometries and materials more precisely to enable a more targeted influence on anisotropic springback and wrinkling. For the round geometry in particular, choosing blank holder forces in MD and CD based on tensile test data recorded in MD and CD is a promising option.

The results revealed a strong influence of segment-specific blank holder force on material flow. The effects of the altered material flow can usually only be understood in retrospect, based on the resulting wrinkling effects. Using the transparent tool enabled a significantly more detailed analysis of the material flow during the forming process. Prior rasterization of the samples and use of a digital image correlation (DIC), as presented in [BRU25], can provide valuable information for this purpose. The continuous recording of the material flow during the experiment can be compared with the material flow in numerical simulations. Such simulations also enable analysis of local stresses and strains in the material. In the case of the rotationally symmetric geometry, the shift in the locations where cracks occur indicates that the stress distribution within the flange area can have a decisive impact on formability and can be influenced by an appropriate choice of segment-wise blank holder forces. Further investigations into this phenomenon require rasterization and DIC or numerical simulations.

Local surface pressure, which is locally affected by wrinkling, has been shown to be another significant factor. Further investigations can analyze local surface pressure for both conventional and segmented blank holders using pressure-sensitive films. This method makes it possible to reliably draw conclusions about actual local surface pressures and the possible influence of segmentation.

Additionally, previous tests have selected a constant blank holder force across the drawing depth to keep the testing volume reasonable. The segmentation and the individual pressure controller provide the opportunity to adjust the blank holder force by segment over the drawing depth. In this case, having a different force distribution across the drawing depth in straight and corner areas may improve wrinkling. Due to the large open test space, it is beneficial to conduct a numerical investigation of optimized force distributions and changes over the drawing depth.

A comparison of the effects of rotationally symmetrical contours and rectangles shows that segmented blank holders improve forming, especially for complex contours. Therefore, in the future, complex contours that quickly reach their limits with conventional blank holders should be used to identify the potential of segmented blank holders.

CONCLUSIONS

1. Deep drawing of paper using a segmented blank holder is possible, but it does not improve forming quality if the force applied to each segment is identical. Improved quality can be achieved by adjusting the load distribution according to the geometry and material.
2. With a round geometry, reducing anisotropy requires applying a higher load in the machine direction (MD). However, this improvement in rotational symmetric components can lead to a deterioration in the wrinkle pattern in CD.
3. With a rectangular geometry, it is possible to adjust the wrinkle pattern, springback,

and the remaining flange length. Applying a higher force to the straight sections than to the corner areas results in completely wrinkle-free areas and a uniform remaining flange length around the circumference. The springback of the straight areas is also reduced.

4. The effects achieved by segmentation were found to be much more pronounced with dry papers than with moistened papers. This was likely due to the coarser wrinkle formation in dry material.
5. The transitions between the segments sometimes cause wrinkling, but do not negatively affect the failure behavior due to the small gap size. The control of the segments by pneumatic cylinders is suitable in terms of the force range and design (size and arrangement) to influence the material feed for dry and moist samples.

ACKNOWLEDGMENTS

The investigations presented in this paper were carried out within the research project DFG GR 1818/85-1 "Controlling the wrinkling of fiber-based materials through adaptive process control and camera-based data acquisition in transparent forming tools." The authors wish to thank the German Research Foundation (DFG) for supporting the project.

REFERENCES CITED

Allwood, J. M., Duncan, S. R., Cao, J., Groche, P., Hirt, G., Kinsey, B., Kuboki, T., Liewald, M., Sterzing, A., and Tekkaya, A. E. (2016). "Closed-loop control of product properties in metal forming," *CIRP Annals* 65(2), 573-596. https://doi.org/10.1016/j.cirp.2016.06.002

Brunk, C., and Groche, P. (2025). "*In-situ* process monitoring in deep-drawing of paper using partially transparent tools," *TAPPI Journal* 24(8), 397-405. https://doi.org/10.32964/TJ24.8.397

Economist Impact and The Nippon Foundation (2021). *Plastics Management Index: Evaluating Effective Management and Sustainable Use of Plastics*, (https://backtoblueinitiative.com/wp-content/uploads/2021/09/Plastics-Management-Index-Whitepaper_sep29.pdf).

Franke, W., Stein, P., Dörsam, S., and Groche, P. (2018). "Formability of paperboard during deep-drawing with local steam application," in: *Proceedings of the 21st International ESAFORM Conference on Material Forming (ESAFORM 2018),* Palermo, Italy, 100008.

Groche, P., Franke, W., and Ackermann, A. (2017). "Ansätze zur verbesserten Umformung von Papier/Approaches to improved forming of paper," *wt Werkstattstechnik online* 107(10), 714-718. https://doi.org/10.37544/1436-4980-2017-10-36

Hauptmann, M. (2010). *Die gezielte Prozessführung und Möglichkeiten zur Prozessüberwachung beim mehrdimensionalen Umformen von Karton durch Ziehen*, Ph. D. Dissertation, Technische Universität Dresden, Dresden.

Hauptmann, M., Kustermann, T., Schmalholz, M., Haug, H., and Majschak, J.-P. (2017).

"Examination of the transferability of technological key features of paperboard deep drawing towards the application in fast-running packaging machines," *Packaging Technology and Science* 30, 21-31. https://doi.org/10.1002/pts.2270

Hauptmann, M., Weyhe, J., and Majschak, J.-P. (2016). "Optimisation of deep drawn paperboard structures by adaptation of the blank holder force trajectory," *Journal of Materials Processing Technology* 232, 142-152. https://doi.org/10.1016/j.jmatprotec.2016.02.007

Huang, H., Lv, Q., Li, L., Xu, Y., Liu, C., Zhang, T., and Liu, Z. (2023). "Individually segmented blank holding system driven by electromagnetics for stamping: Modeling, validation, and prototype," *Journal of Materials Processing Technology* 313, 117883. https://doi.org/10.1016/j.jmatprotec.2023.117883

Jessen, N., and Groche, P. (2025). "Higher drawing depth and less wrinkling due to drawbeads in paperboard forming," *BioResources* 20(1), 1399-1412. https://doi.org/10.15376/biores.20.1.1399-1412

Jessen, N., Schetle, M., and Groche, P. (2022). "Numerical analysis of the deep drawing process of paperboards at different humidities," *WGP Tagungsband*, 131-141. https://doi.org/10.1007/978-3-031-18318-8_14

Müller, T., Lenske, A., Hauptmann, M., and Majschak, J.-P. (2017). "Analysis of dominant process parameters in deep-drawing of paperboard," *BioResources* 12(2), 3520-3545. https://doi.org/10.15376/biores.12.2.3530-3545

Stora Enso (2025). *Trayforma – Datasheet Technical Specification*, (https://www.storaenso.com/-/media/documents/download-center/documents/product-specifications/paperboard-materials/trayforma-en.pdf).

Vogt, L., and Hauptmann, M. (2025). "Tailoring thermal energy supply towards the advanced control of deformation mechanisms in 3D forming of paper and board," *JMMP* 9(5), article 142. https://doi.org/10.3390/jmmp9050142

Wallmeier, M., Noack, K., Hauptmann, M., and Majschak, J.-P. (2016). "Shape accuracy analysis of deep drawn packaging components made of paperboard," *Nordic Pulp and Paper Research Journal* 31, 323-332. https://doi.org/10.3183/npprj-2016-31-02-p323-332

Yagami, T., Manabe, K., Yang, M., and Koyama, H. (2004). "Intelligent sheet stamping process using segment blankholder modules," *Journal of Materials Processing Technology* 155-156, 2099-2105. https://doi.org/10.1016/j.jmatprotec.2004.04.144

Zhang, H., Qin, S., and Cao, L. (2021). "Investigation of the effect of blank holder force distribution on deep drawing using developed blank holder divided into double rings," *Journal of the Brazilian Society of Mechanical Sciences and Engineering* 43(6). https://doi.org/10.1007/s40430-021-03003-7

Article submitted: November 27, 2025; Peer review completed: January 24, 2026; Revised version received and accepted: January 30, 2026; Published: February 4, 2026.
DOI: 10.15376/biores.21.2.2832-2850